

Supporting Information for

Photoluminescent and pH-Responsive Supramolecular Structures from Co-assembly of Carbon Quantum Dots and Zwitterionic Surfactant Micelles

Xiaofeng Sun,^{a,d} Mengjun Chen,^b Yiqiang Zhang,^{a,c} Yanji Yin,^{a,c} Linwen Zhang,^{a,d} Hongguang Li^{a*}
and Jingcheng Hao^{b*}

^a *State Key Laboratory of Solid Lubrication & Laboratory of Clean Energy Chemistry and Materials, Lanzhou Institute of Chemical Physics, Chinese Academy of Sciences, Lanzhou, Gansu Province, 730000, China;*

^b *Key Laboratory of Colloid and Interface Chemistry & Key Laboratory of Special Aggregated Materials, Shandong University, Ministry of education, Jinan, Shandong Province, 250100, China;*

^c *China Research Institute of Daily Chemical Industry, Taiyuan, 030001, China;*

^d *University of Chinese Academy of Sciences, Beijing, 100049, China.*

* Corresponding authors: Prof. Hongguang Li E-mail: hgli@licp.cas.cn

Phone: +86-931-4968829. Fax: +86-931-4968163.

Prof. Jingcheng Hao E-mail: jhao@sdu.edu.cn

Phone: +86-531-88366074. Fax: +86-531-88364750.

Calculation of surface carboxyl moieties density of CQDs

The mean diameter of the CQDs was determined by HRTEM to be 2.0 nm (Fig. 1C), thus the volume of each CQD (V) can be obtained according to equation 1:

$$V = \frac{4}{3} \pi R^3 = \frac{4}{3} \times 3.14 \times 1.0^3 = 4.19 \text{ nm}^3 \quad (1)$$

Assuming that the density of the CQDs (ρ) equals $1.8 \text{ g}\cdot\text{cm}^{-3}$, the quality of each CQD (m) can be calculated according to equation 2:

$$m = \rho V = 1.8 \times 4.19 \times 10^{-21} = 7.54 \times 10^{-21} \text{ g} \quad (2)$$

For an aqueous solution of CQDs with a concentration of $0.1 \text{ mg}\cdot\text{mL}^{-1}$ ($0.1 \text{ g}\cdot\text{L}^{-1}$) and a volume of 1 L, the total number of CQDs is:

$$N_{\text{CQDs}} = \frac{0.1}{7.54 \times 10^{-21}} = 1.33 \times 10^{19}$$

For an aqueous solution of CQDs with a concentration of $0.1 \text{ mg}\cdot\text{mL}^{-1}$ ($0.1 \text{ g}\cdot\text{L}^{-1}$) and a volume of 1 L, 1.0-1.2 mmol TTAB is needed to get the maximum amount of precipitates. If 1.0 mmol is taken, the total number of negative charges is:

$$n^- = 1.0 \times 10^{-3} \times 1.0 \times 6.02 \times 10^{23} = 6.02 \times 10^{20}$$

The number of negative charges on each CQD is:

$$N^- = \frac{6.02 \times 10^{20}}{1.33 \times 10^{19}} = 45.26$$

The surface charge density is:

$$\sigma^- = \frac{45.26}{4 \times 3.14 \times 1.0^2} = 3.60 \text{ nm}^{-2}$$

Similarly, if 1.2 mmol TTAB is taken, N^- and σ^- can be calculated to be 54.31 and 4.32, respectively.

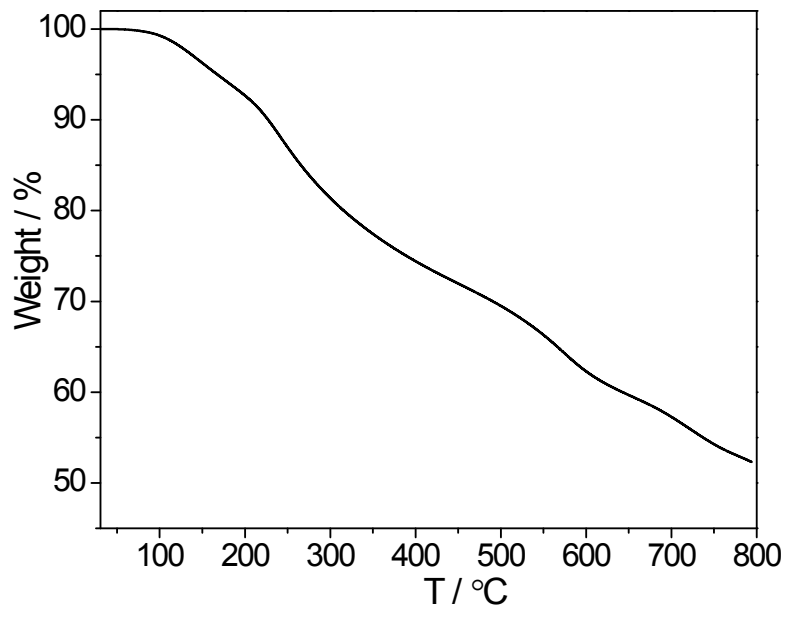


Fig. S1 TGA curve of the CQDs.

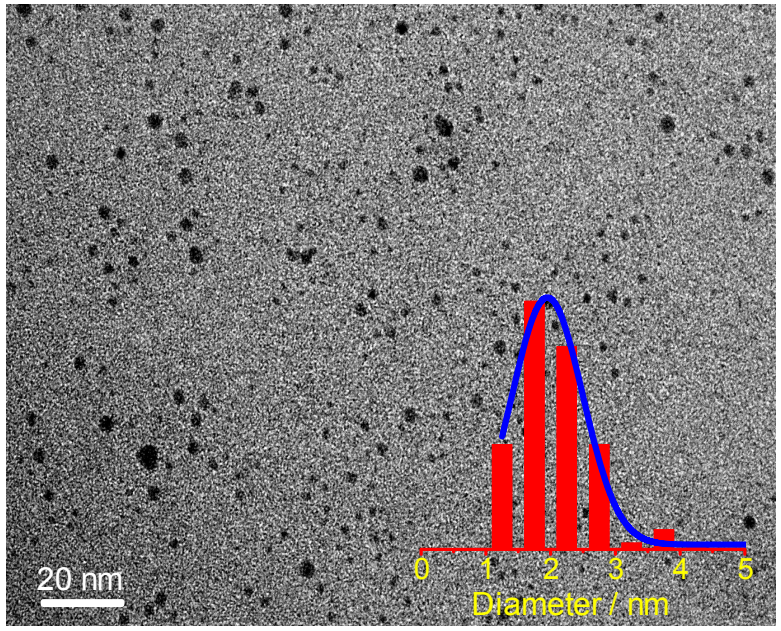


Fig. S2 HRTEM image of the CQDs. Inset is the size distribution.

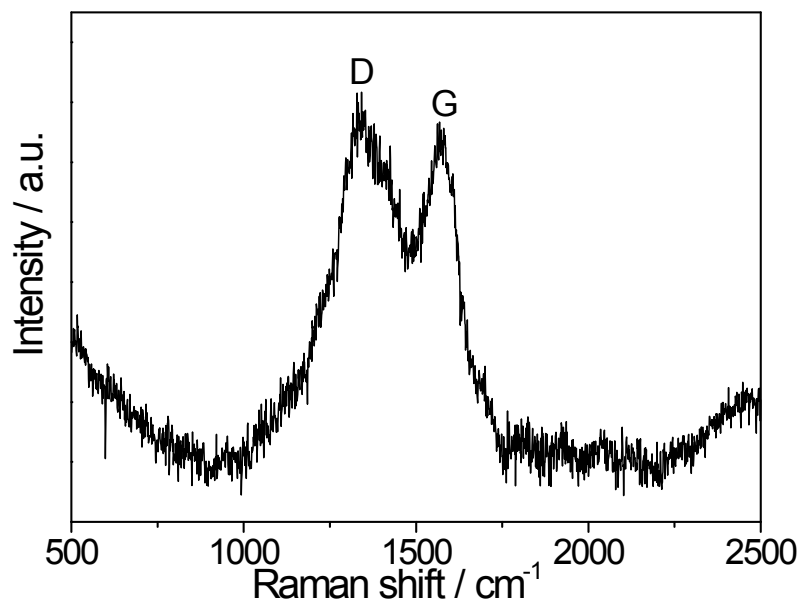


Fig. S3 Raman spectra of the CQDs.

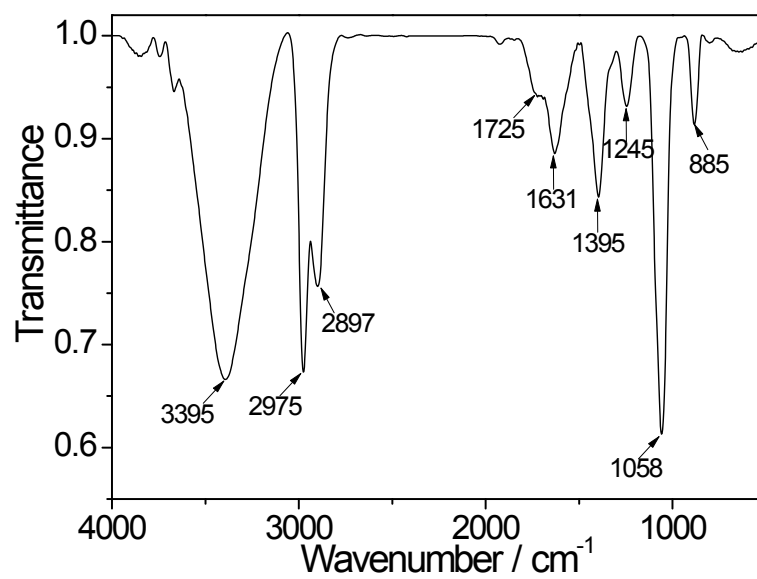


Fig. S4 FTIR spectra of the CQDs.

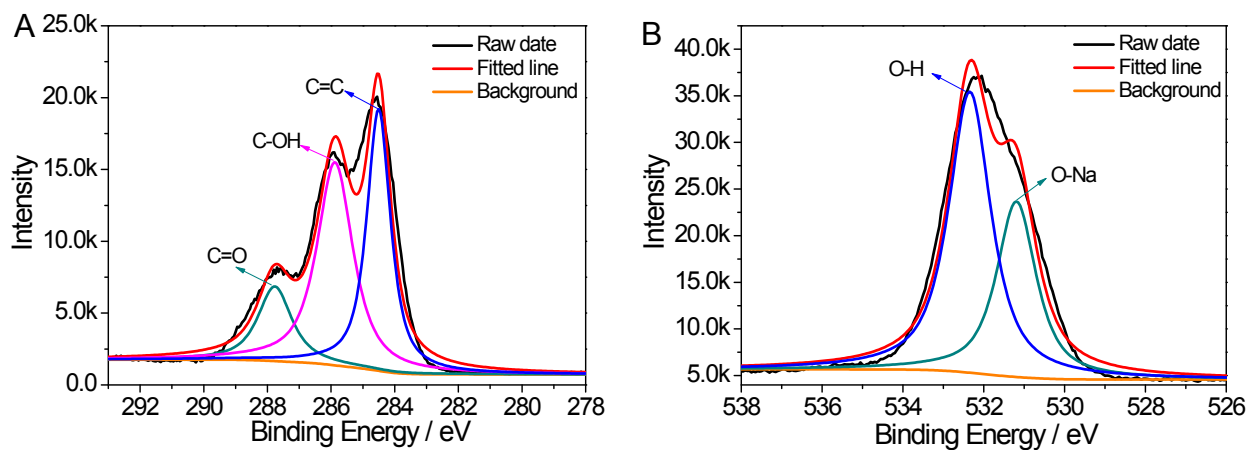


Fig. S5 High-resolution XPS C1s (A) and O1s (B) spectra of the CQDs. Each band was deconvoluted.

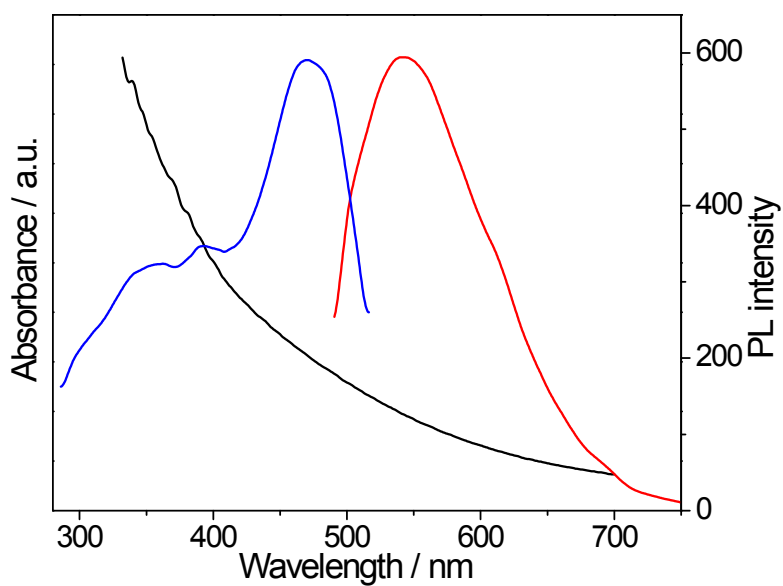


Fig. S6 UV-vis absorbance (black line), the optimal excitation (blue line) and emission (red line) PL spectra of an aqueous solution of as-prepared CQDs (0.1 mg·mL⁻¹).

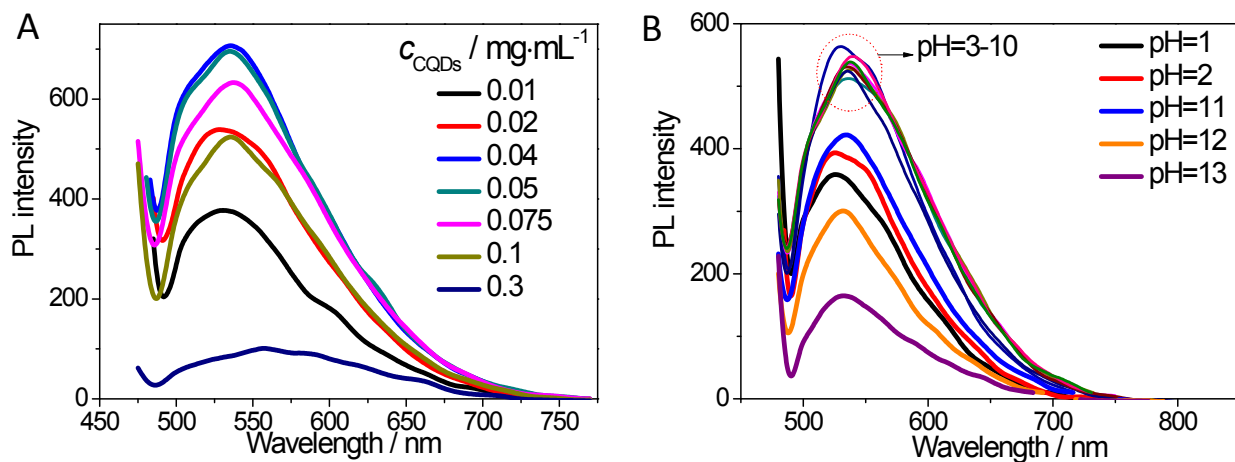


Fig. S7 A) Emission spectra at $\lambda_{\text{ex}} = 470$ nm as a function of c_{CQDs} . B) Emission spectra at $\lambda_{\text{ex}}=470$ nm as a function of pH. The concentration of CQDs is $0.1 \text{ mg}\cdot\text{mL}^{-1}$.

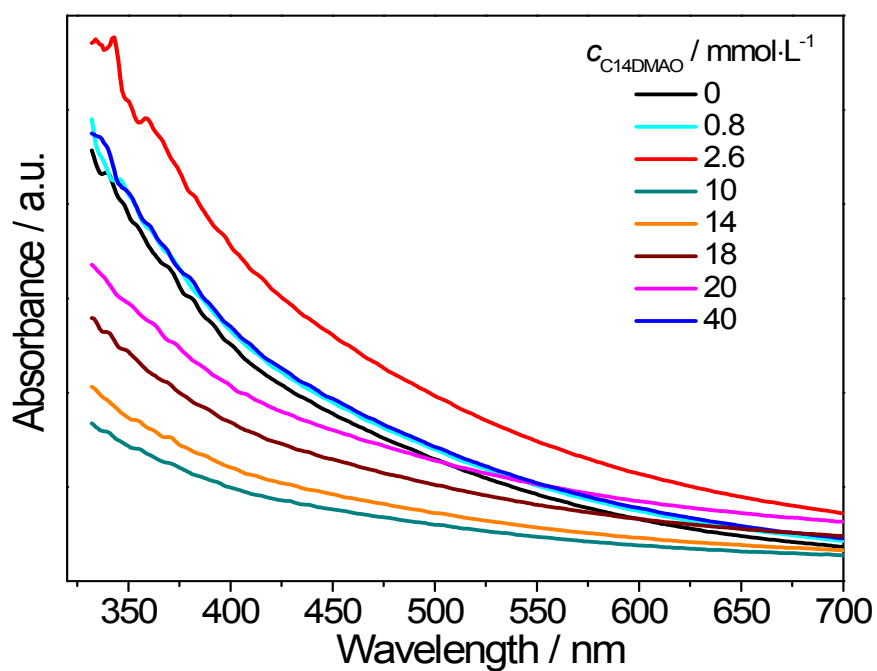


Fig. S8 The absorption spectra as a function of c_{C14DMAO} . The concentration of CQDs is $0.1 \text{ mg}\cdot\text{mL}^{-1}$.

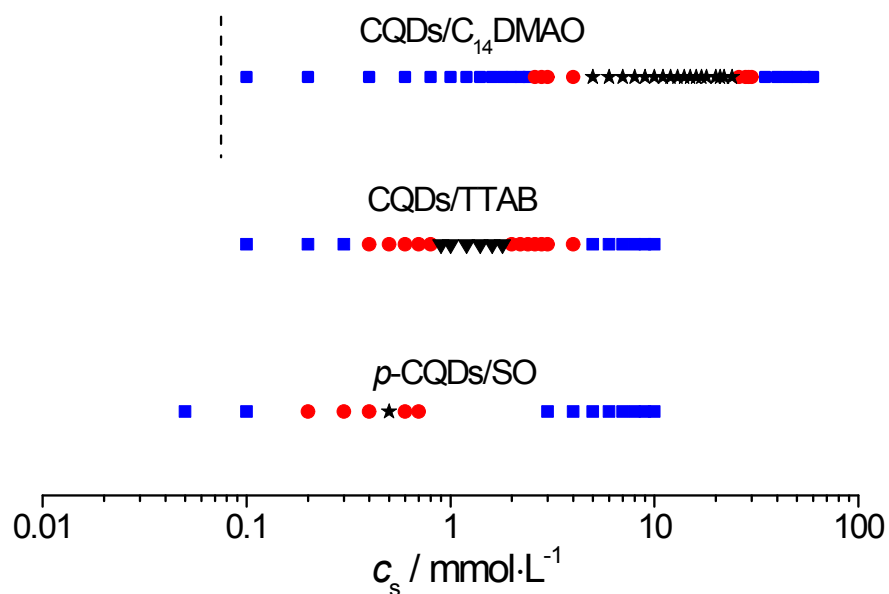


Fig. S9 Phase sequence of 0.1 mg·mL⁻¹ CQDs used in current study mixed with increasing amount of C₁₄DMAO or TTAB. For comparison, the phase sequence of 0.5 mg·mL⁻¹ *p*-CQDs mixed with increasing amount of sodium oleate (SO) is also given. Squares: isotropic phase. Circles: turbid phase. Pentagons: phase separated region.

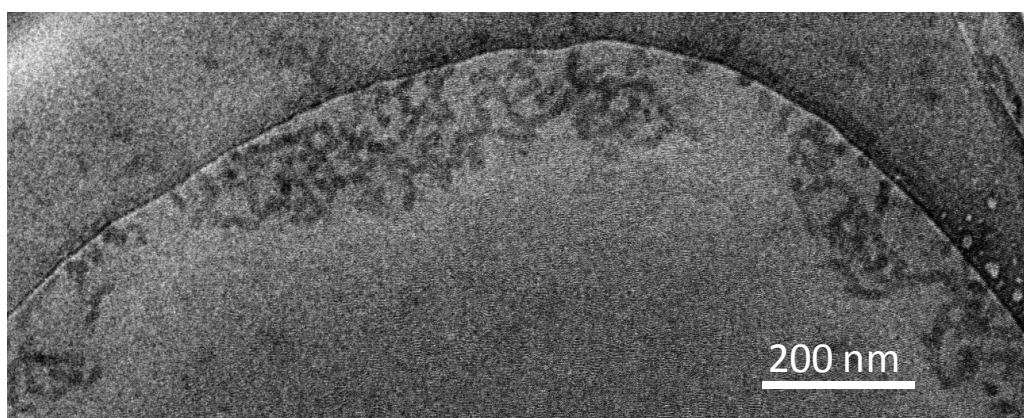


Fig. S10 Cryo-TEM image of the self-assemblies formed at $c_{\text{C}_{14}\text{DMAO}} = 0.6$ mmol·L⁻¹.

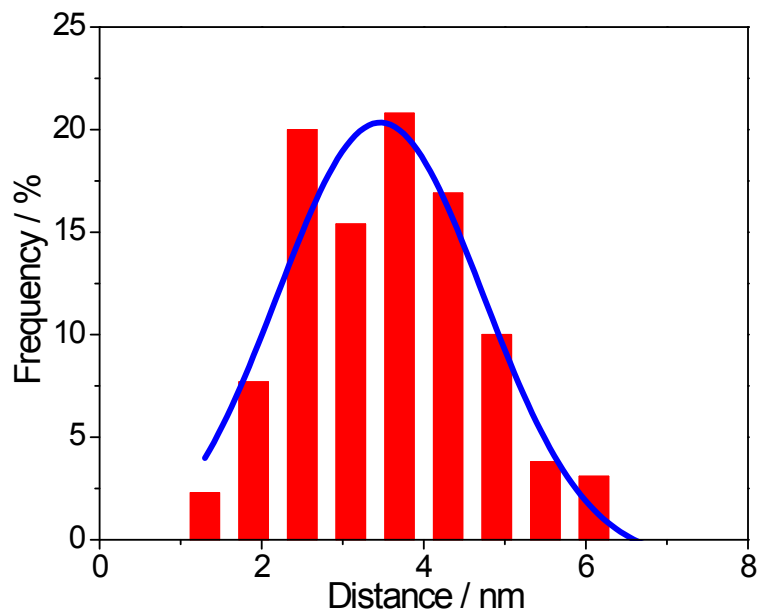


Fig. S11 Distribution of the distance between adjacent CQDs within the skeletons of the supramolecular polymer formed in the sample with $c_{\text{C14DMAO}} = 0.6 \text{ mmol}\cdot\text{L}^{-1}$.

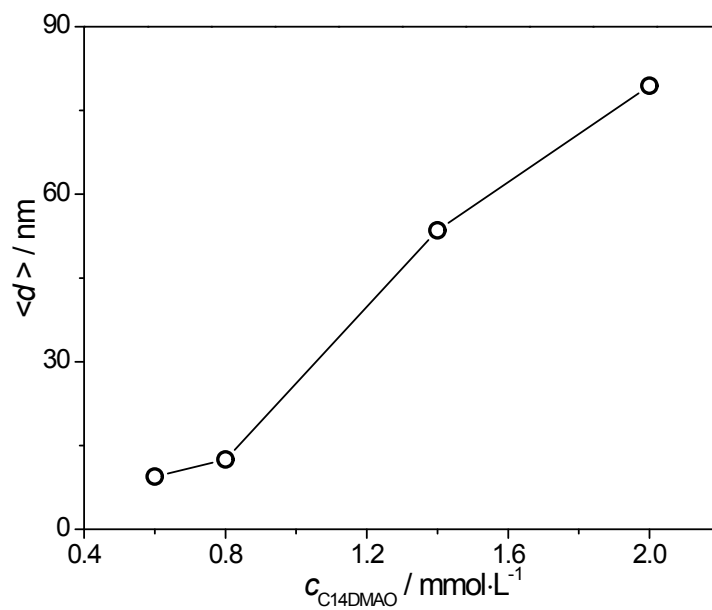


Fig. S12 Statistics of the mean diameter ($\langle d \rangle$) of the supramolecular polymers and ribbons formed in the I_1 region.

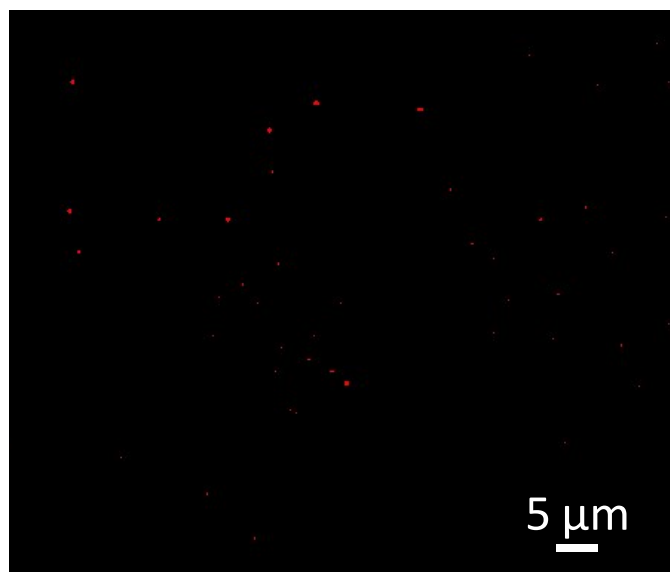


Fig. S13 A typical confocal fluorescence microscopy image of the vesicles formed in the sample with $c_{\text{C14DMAO}} = 2.6 \text{ mmol}\cdot\text{L}^{-1}$.

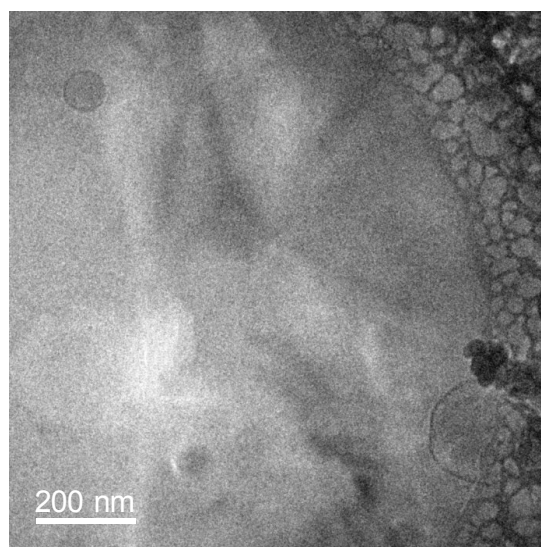


Fig. S14 A typical cryo-TEM image of the vesicles formed in the sample with $c_{\text{C14DMAO}} = 2.6 \text{ mmol}\cdot\text{L}^{-1}$.

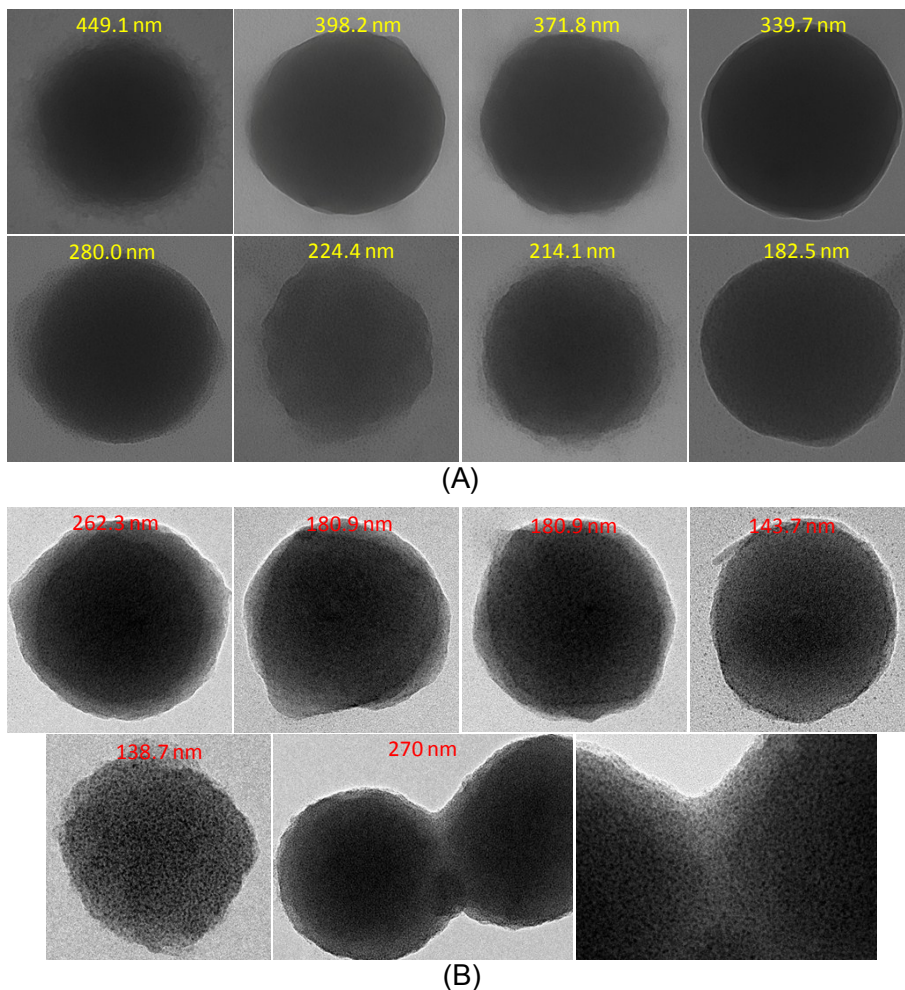


Fig. S15 TEM (A) and HRTEM (B) images of the vesicles with varying sizes as indicated in the aged sample with $c_{C_{14}DMAO} = 2.6 \text{ mmol}\cdot\text{L}^{-1}$. In B, a vesicle dimer is also shown together with the magnified image in the junction.

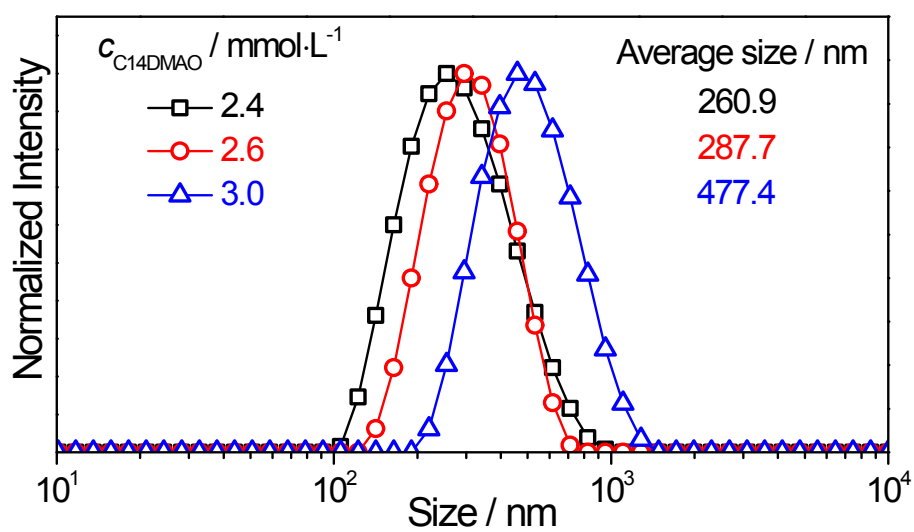


Fig. S16 Size distribution of the self-assemblies from in the three typical samples with different $c_{C_{14}DMAO}$ as indicated.

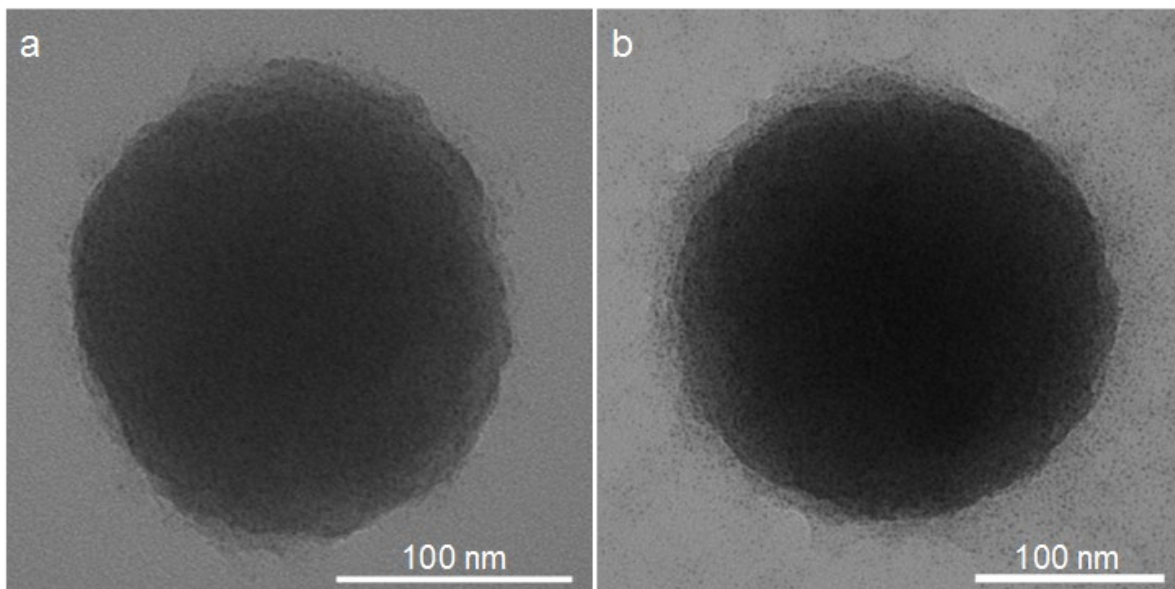


Fig. S17 Typical TEM images of the vesicles formed in the samples with c_{C14DMAO} to be 2.4 (a) and 3.0 (b) $\text{mmol}\cdot\text{L}^{-1}$, respectively.

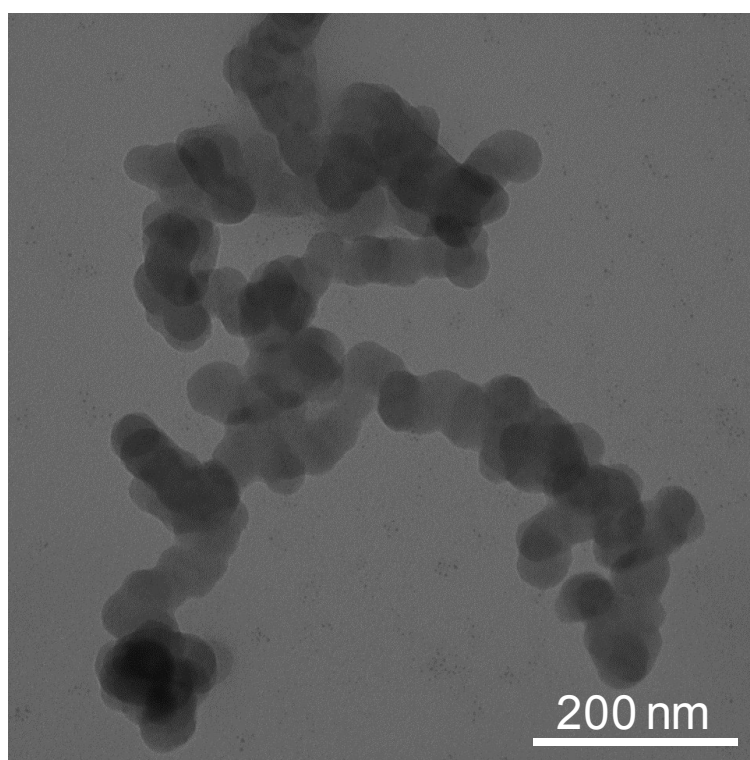


Fig. S18 A typical TEM image of the self-assemblies formed in the sample with $c_{\text{C14DMAO}} = 26$ $\text{mmol}\cdot\text{L}^{-1}$.

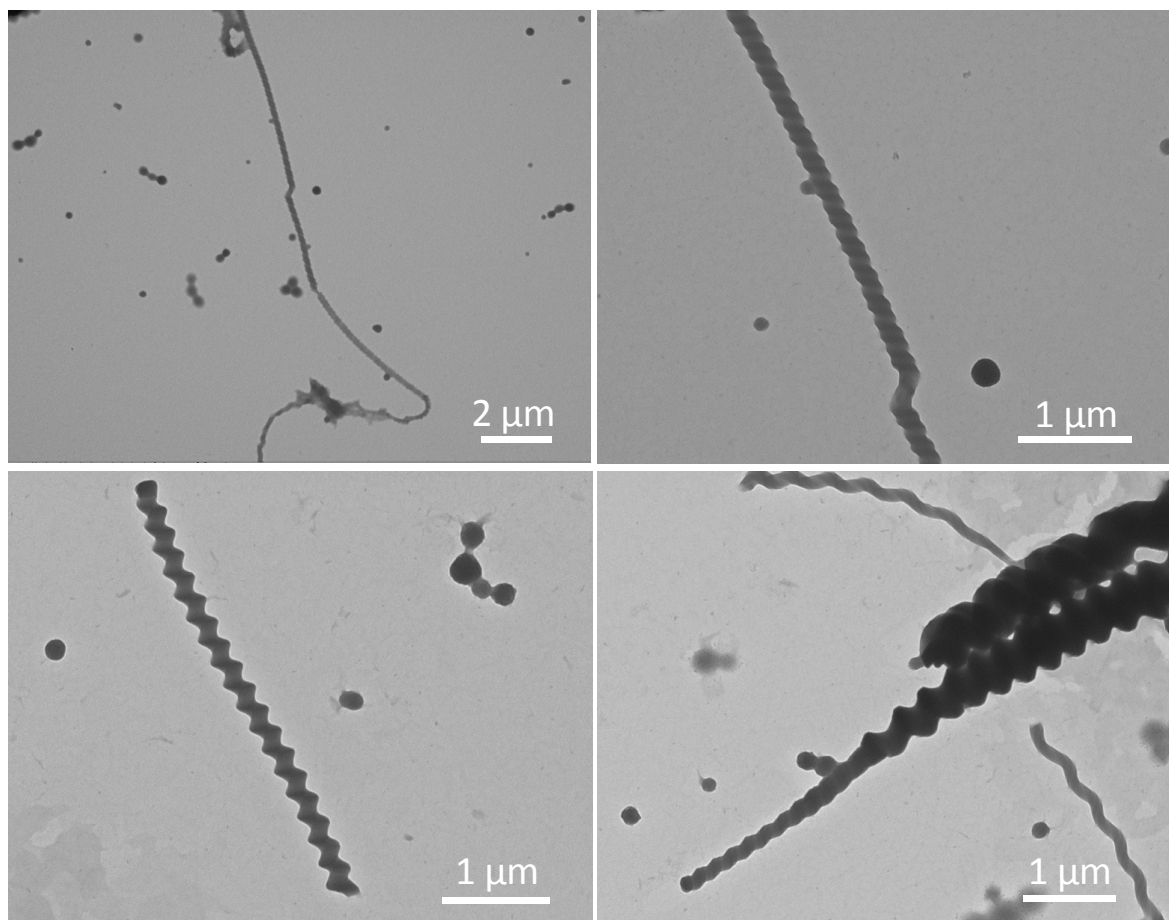


Fig. S19 TEM images of the self-assemblies observed in the sample with $c_{\text{C}_{14}\text{DMAO}} = 2.6 \text{ mmol}\cdot\text{L}^{-1}$ after the first circle of NaOH-HCl titration (0.16 eq each). Helices were observed.

Data notion:

By observations on parallel samples, we realized that the helices, though have been clearly detected, are the minority and the majority are still vesicles. The reason could be that the arrangement of the vesicles in strictly one-dimension is quite difficult, as pointed out already in the maintext. Future work should be the introduction of magnetic or electronic component into the system, which can help to align the vesicles through applying a magnetic or electric field.

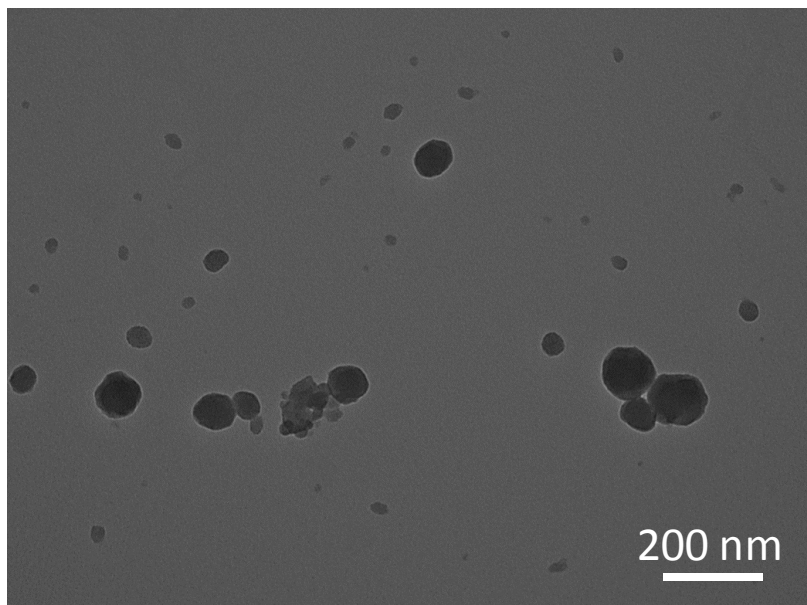


Fig. S20 TEM image of $2.6 \text{ mmol}\cdot\text{L}^{-1}$ C_{14}DMAO at low amount of HCl (0.32 eq).

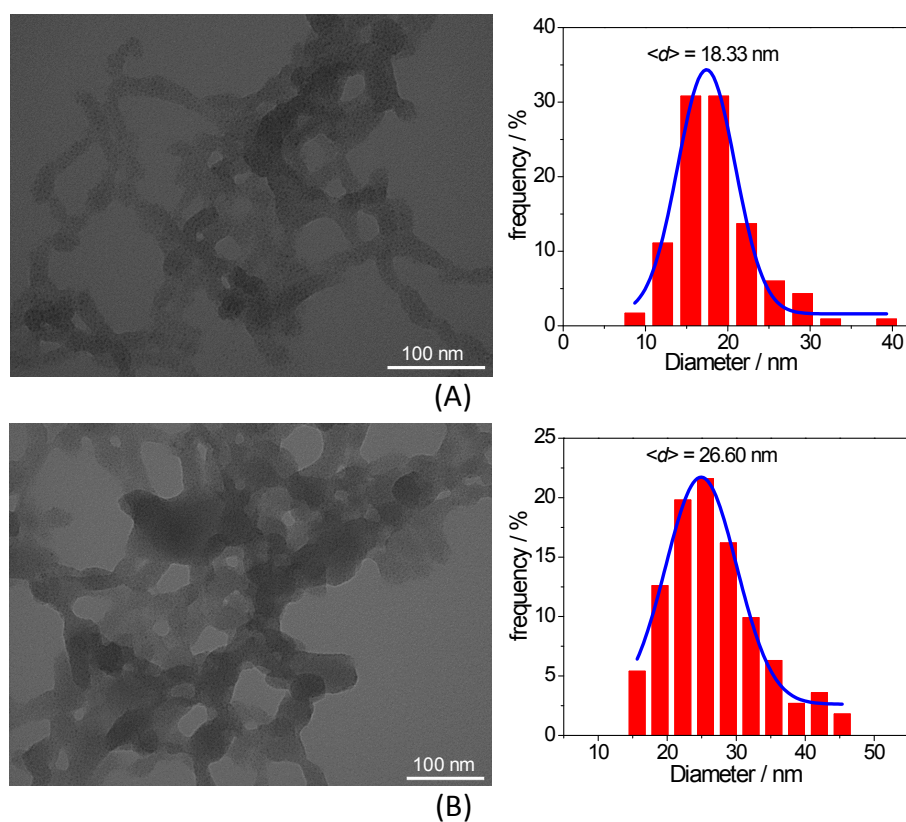


Fig. S21 TEM image of the supramolecular polymer and corresponding size distribution of the skeletons formed at $c_{\text{C}_{14}\text{DMAO}} = 0.8 \text{ mmol}\cdot\text{L}^{-1}$ after the addition of 0.2 eq (A) and 0.4 eq (B) HCl.

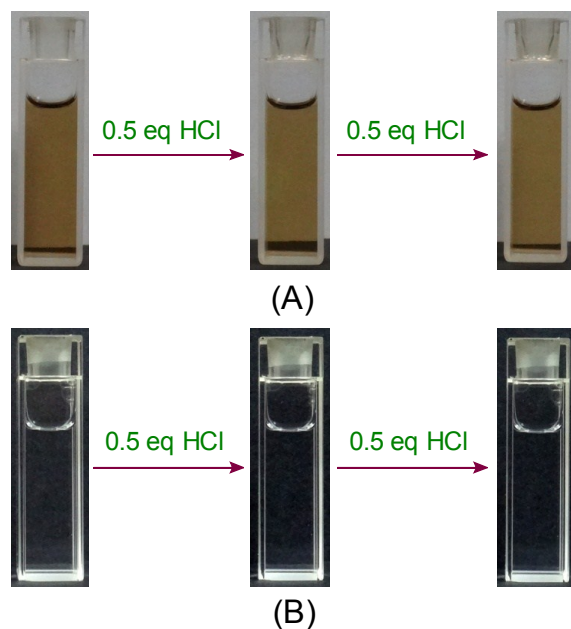


Fig. S22 Changes of the appearance of $0.1 \text{ mg}\cdot\text{mL}^{-1}$ CQDs (A) and $0.8 \text{ mmol}\cdot\text{L}^{-1}$ C_{14}DMAO (B) upon the addition of HCl.

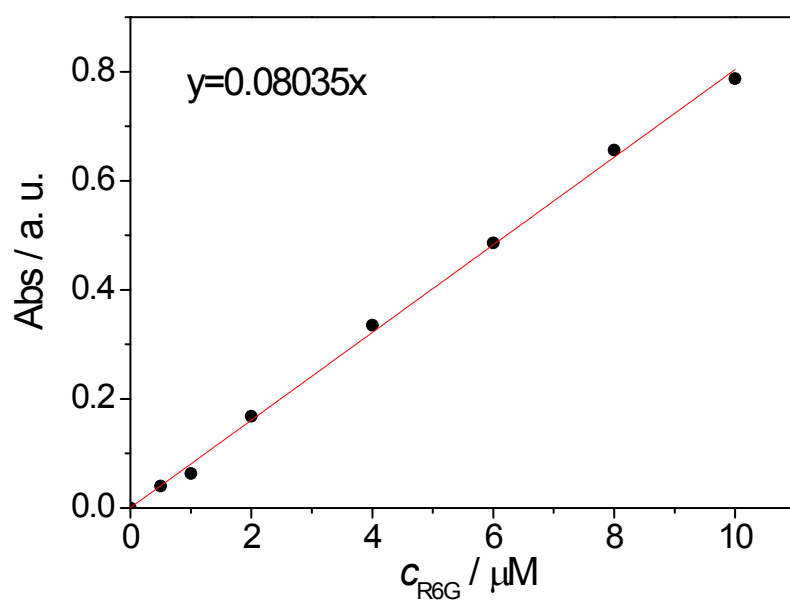


Fig. S23 The UV calibration curve of R6G aqueous solution at 526 nm.